

pubs.acs.org/JACS Article

Metal-Mediated, Autolytic Amide Bond Cleavage: A Strategy for the Selective, Metal Complexation-Catalyzed, Controlled Release of Metallodrugs

Dariusz Śmiłowicz, Shawn Eisenberg, Rochelle LaForest, Jennifer Whetter, Annapoorani Hariharan, Jake Bordenca, Christopher J. Johnson, and Eszter Boros*



Cite This: J. Am. Chem. Soc. 2023, 145, 16261-16270



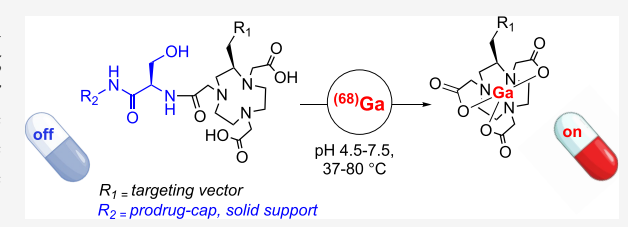
ACCESS I

III Metrics & More

Article Recommendations

Supporting Information

ABSTRACT: Activation of metalloprodrugs or prodrug activation using transition metal catalysts represents emerging strategies for drug development; however, they are frequently hampered by poor spatiotemporal control and limited catalytic turnover. Here, we demonstrate that metal complex-mediated, autolytic release of active metallodrugs can be successfully employed to prepare clinical grade (radio-)pharmaceuticals. Optimization of the Lewis-acidic metal ion, chelate, amino acid linker, and biological targeting vector provides



means to release peptide-based (radio-)metallopharmaceuticals in solution and from the solid phase using metal-mediated, autolytic amide bond cleavage (MMAAC). Our findings indicate that coordinative polarization of an amide bond by strong, trivalent Lewis acids such as Ga³⁺ and Sc³⁺ adjacent to serine results in the N, O acyl shift and hydrolysis of the corresponding ester without dissociation of the corresponding metal complex. Compound [⁶⁸Ga]Ga-10, incorporating a cleavable and noncleavable functionalization, was used to demonstrate that only the amide bond-adjacent serine effectively triggered hydrolysis in solution and from the solid phase. The corresponding solid-phase released compound [⁶⁸Ga]Ga-8 demonstrated superior in vivo performance in a mouse tumor model compared to [⁶⁸Ga]Ga-8 produced using conventional, solution-phase radiolabeling. A second proof-of-concept system, [⁶⁷Ga]Ga-17A (serine-linked) and [⁶⁷Ga]Ga-17B (glycine-linked) binding to serum albumin via the incorporated ibuprofen moiety, was also synthesized. These constructs demonstrated that complete hydrolysis of the corresponding [⁶⁸Ga]Ga-NOTA complex from [⁶⁷Ga]Ga-17A can be achieved in naïve mice within 12 h, as traceable in urine and blood metabolites. The glycine-linked control [⁶⁸Ga]Ga-17B remained intact. Conclusively, MMAAC provides an attractive tool for selective, thermal, and metal ion-mediated control of metallodrug activation compatible with biological conditions.

■ INTRODUCTION

Clinically viable prodrugs require close spatiotemporal control and release of activated, potent drug molecules at the site of interest. Common bond cleavage strategies incorporate triggers such as pH, UV irradiation, or enzyme proteolysis to modulate drug selectivity, function, and pharmacokinetics. However, dependence of exogenous triggers and their relative abundance in the extracellular milieu can drastically limit applicability and drug efficacy. P-12

Stimulus-responsive prodrugs that involve metal ions can exhibit similar limitations, where efficient prodrug activation with external stimuli and close control of pharmacokinetics remains challenging and therefore represents a current area of research interest. Strategies such as transition metal-mediated, 16–18 cell-compatible catalysis, 19–21 or photodynamic triggering for drug activation or release have shown efficacy. However, the dependence on an external stimulus or catalyst concentration can pose significant limitations on the accessibility or threshold abundance of the biological target. Specifical strategies where the dependence of the biological target.

Selective, metal ion-mediated amide bond cleavage is a well-characterized process in nature: a range of metalloproteases exist and exhibit great specificity and efficacy in aqueous media and ambient temperature. Inspired by these metalloenzymes, Groves and Baron and Hegg and Burstyn demonstrated that Co³⁺ and Cu²⁺ small-molecular chelate systems were capable of amide bond scission via formation of a metal-bound, ternary hydroxo ligand acting as a nucleophile. More recently, Bal and coworkers employed Ni²⁺ chelating peptides that were selectively cleaved adjacent to serine by the N, O acyl shift and subsequent ester hydrolysis, S5,36 a process also viable using Lewis-acidic V-oxo species and Sc³⁺. However, these systems relied on excess

Received: May 25, 2023 Published: July 12, 2023





(Metallo)drug activation aproaches (previous work):

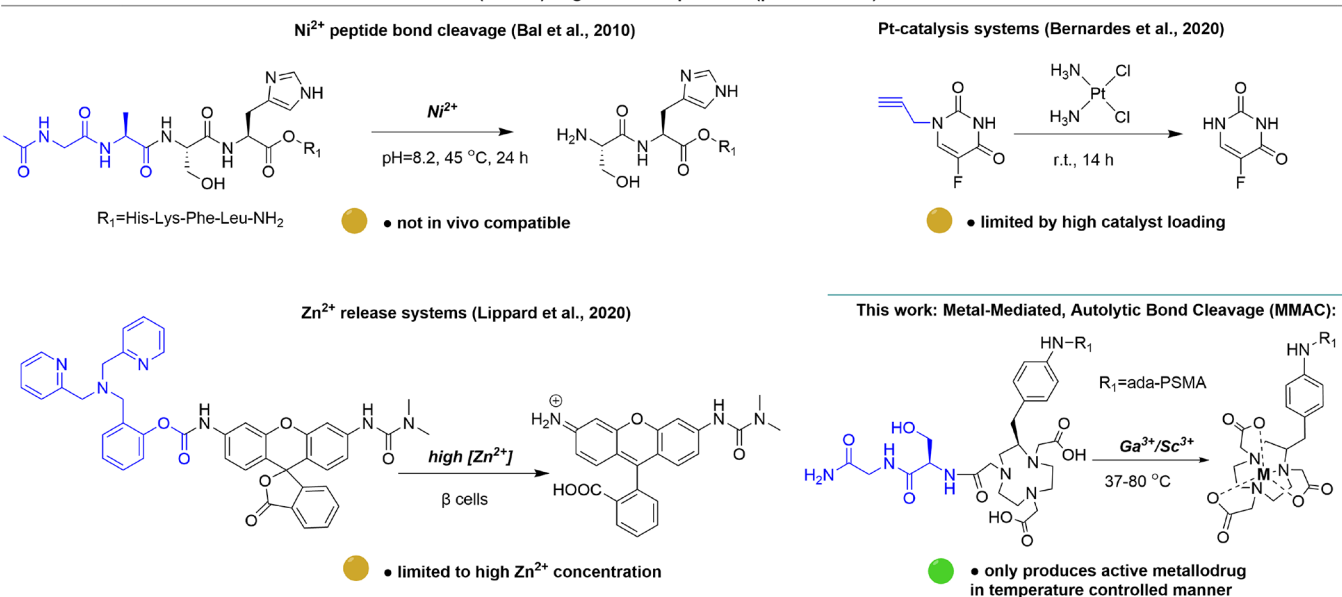


Figure 1. Summary of previously employed metal ion-mediated bond cleavage and prodrug activation approaches reported in the literature; all rely on labile metal ion binding and bimolecular reaction mechanisms, which are inherently limiting in vivo. This is not the case for MMAAC, which does not depend on the exogenous catalyst concentration and proceeds with an autolytic mechanism. Structural components denoted in blue are cleaved/hydrolyzed in response to the catalyst/metal ion binding stimulus.

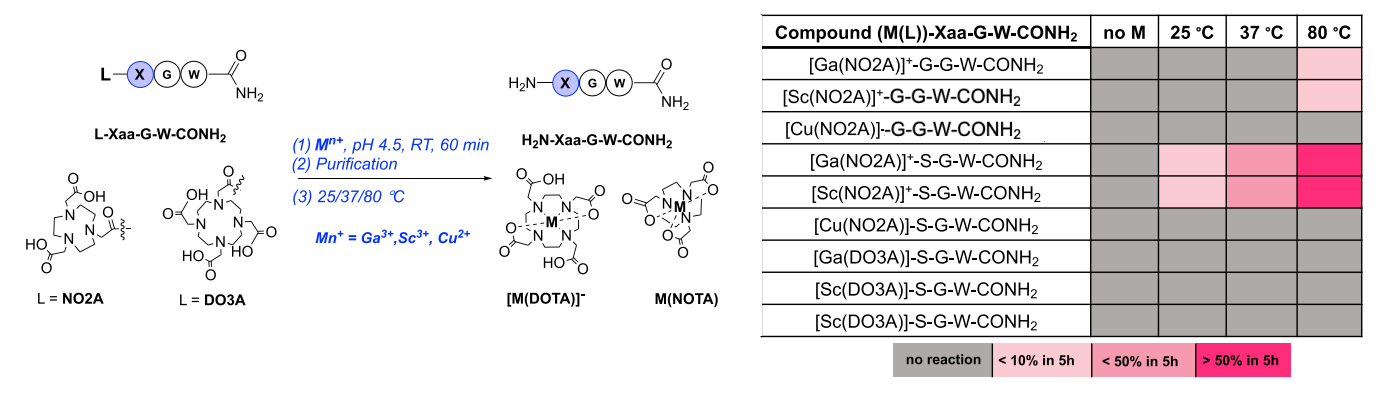


Figure 2. Model peptide—chelate conjugates and corresponding metal complexes screened for autolytic amide bond cleavage activity producing a cleaved, chelate-adjacent amide bond to release the metal chelate and tripeptide. The complex-adjacent amino acid X = G (glycine) and S (serine) was varied to probe the sequence dependence of reactivity.

metal aqua-ion in solution or hemilabile coordination complexes to conduct bimolecular bond cleavage reactions, which compromises their utility for controlled prodrug activation and release under trace or in vivo conditions (Figure 1).^{38–41}

Here, we report the development, optimization, and in vivo validation of metal-mediated, autolytic amide bond cleavage (MMAAC), a modular approach for the selective metal complexation-induced release and activation of metallodrugs. Using a model system, we elucidate the optimal combination of the peptide sequence, chelate and metal ion, and probe reaction rates at temperatures and pH conditions of interest. Subsequently, we demonstrate the feasibility to release active (radio)pharmaceuticals via MMAAC in solution and from a solid support and in live mice.

■ RESULTS AND DISCUSSION

Initial Screening and Scope. To probe the impact of a metal ion, chelator, and metal complex-adjacent amino acid,

we prepared a modular tripeptide sequence capped by an azamacrocyclic metal chelator on the N-terminus. Specifically, we linked 1,4,7-triazacyclononane-triacetic acid (NOTA) or 1,4,7,10-tetraazacyclododecane-1,4,7,10-tetraacetic acid (DOTA) to H-X-G-W-NH $_2$ (where X=S or G). Tryptophan (W) was incorporated to provide a spectroscopic handle for HPLC monitoring, and G provided an additional short spacer to reduce steric encumbrance around the metal complex. Subsequently, chelation of the Lewis-acidic Ga^{3+} , Sc^{3+} , and Cu^{2+} ions produced model systems for further testing. These ions were selected as they are efficiently chelated by both macrocyclic chelator systems and possess biomedically relevant radioactive isotopes.

Amide bond hydrolysis was induced by complexation by the metal ion at pH 4.5 followed by immediate adjustment of reaction temperature. Reaction progress was monitored using high-performance liquid chromatography and mass spectrometry (HPLC-MS). In the absence of metal ions, model peptides did not hydrolyze at any temperature tested (25, 37, and 80

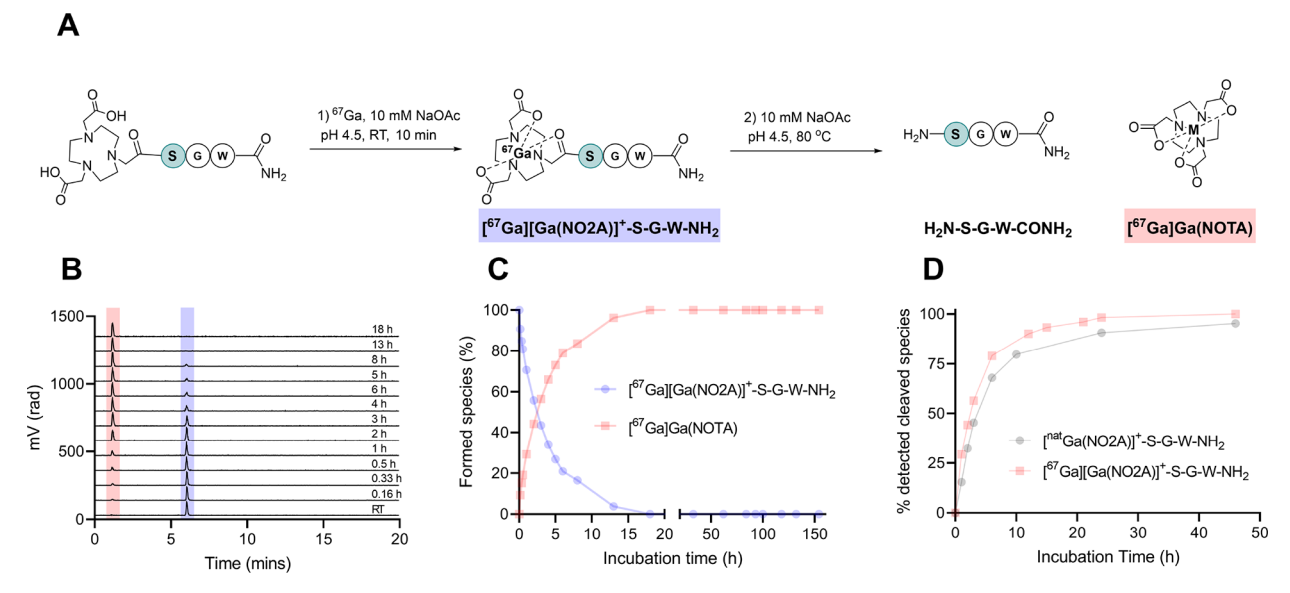


Figure 3. (A) Stepwise radiochemical labeling and reaction scheme to monitor autolytic amide bond cleavage. (B) Stacked chromatograms monitoring the bond cleavage reaction at 80 °C. (C) Quantitation of the reactant and product based on radio-HPLC chromatograms. (D) Comparison of the time course of the macroscopic cleavage reaction and the corresponding reaction at the tracer showing that both reactions show nearly identical kinetics.

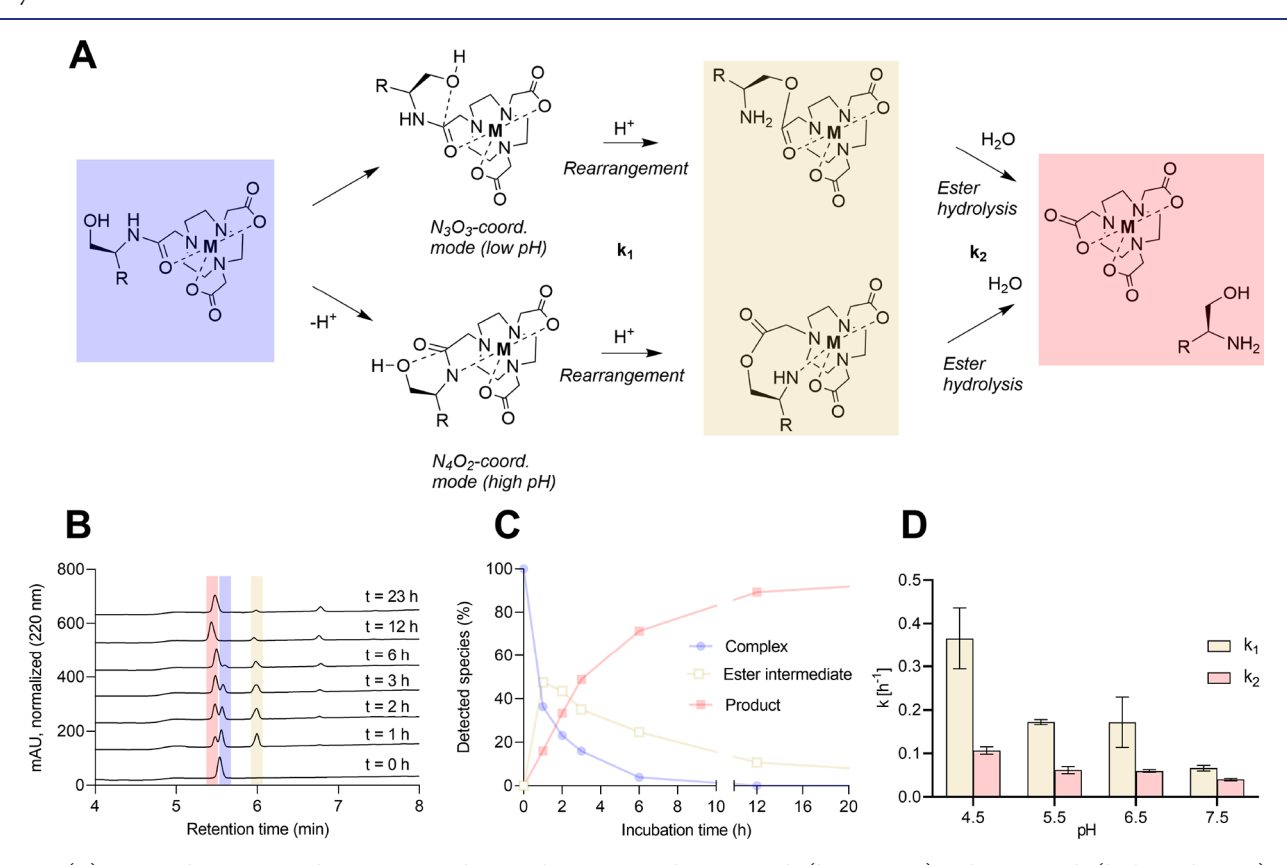


Figure 4. (A) Proposed reaction mechanisms proceeding via the N_3O_3 coordination mode (low pH, top) and N_4O_2 mode (high pH, bottom), with both resulting in the N, O acyl shift followed by ester hydrolysis to form the products. (B) Representative HPLC chromatograms of the reactant (gray box), N, O acyl shifted intermediate (gold box), and cleaved peptide product (red box). (C) Species time course analysis and quantification. (D) Determination of individual reaction rates for rearrangement and hydrolysis reaction (n = 2 and 3). R = GW-CONH₂.

°C). Only slow hydrolysis was observed for $[M(NO2A)]^{n+}$ -G-W-CONH₂ under forcing conditions, while $[M(DO3A)]^{n+}$ -G-G-W-CONH₂ peptides were not hydrolyzed, regardless of the identity of the metal ion. However, $[M(NO2A)]^{n+}$ -S-G-W-NH₂ exhibited observable amide bond hydrolysis for $M = Ga^{3+}$

and Sc^{3+} with accelerating kinetic rates as temperature was increased. All Cu^{2+} complexes tested remained hydrolytically stable within the investigated time frame (Figures S39–S48).

We posit that the investigated DOTA complexes do not involve sufficient amide bond coordination and polarization,

and Cu^{2+} favors formation of a 5-coordinate complex with NO2A without coordinative involvement of the amide, resulting also in decreased bond polarization. [Ga(NO2A-amide)]⁺ and [Sc(NO2A-amide)]⁺ complexes, however, both efficiently catalyzed amide bond hydrolysis adjacent to a serine. Figure 2 summarizes the observed reactivity.

Encouraged by natGa-triggered cleavage, we next probed the selective release of radiolabeled complexes at tracer concentrations, to affirm that the proteolytic activity was governed by the complexed metal ion and not by any free metal ion present in macroscopic excess. The model peptides (10 nmol) were radiolabeled with 100 μ Ci of ⁶⁷Ga (corresponding to 2.5 pmol), at room temperature and pH 4.5 (10 mM sodium acetate). Radiochemical labeling yields (RCY) of >99% were observed for all model peptides at room temperature within 10 min (see Supporting Information, Schemes S4-S6). Following radiochemical complexation, the autolytic cleavage was monitored at different temperatures in accordance with macroscopic, nonradioactive experiments (25, 37, and 80 °C). As anticipated, the [67Ga]Ga(NOTA) complex was released from the conjugate [67Ga][Ga(NO2A)]+-S-G-W-CONH₂. The autolytic amide bond cleavage resulted in clean product formation at 80 °C as well as 37 °C (Figure 3B-D). The corresponding [⁶⁷Ga][M(DOTA)]-S-G-W-CONH₂ control was hydrolytically stable within the investigated time frame (Supporting Information, Figure S55). While corresponding Sc complexes exhibited analogous behavior, radiochemical studies were not conducted with the corresponding radioactive isotope as [Sc(NO2A-amide)]⁺ complexes do not exhibit sufficient kinetic inertness for in vivo applications and drug development.42

Kinetic Studies. As the amide bond cleavage occurs only at appreciable reaction rates with model peptides containing [Ga(NO2A)]⁺-amide and [Sc(NO2A)]⁺-amide linked to a serine, we considered multiple mechanistic pathways involving the metal complex as plausible: (i) activation of a ternary aqua ligand by direct coordination to the metal center, (ii) activation/destabilization of the complex-adjacent peptide bond by coordination of the carbonyl oxygen, and (iii) N, O acyl shift rearrangement involving transient coordination of the alpha-amine of the serine (Figure 4A).³⁸

We performed the cleavage assay at varying pH values of 4.5, 5.5, 6.5, 7.5, and 8.5 at 80 $^{\circ}$ C using the [Ga(NO2A)]⁺-S-G-W-CONH₂ model sequence, which was identified during the structural screening. To monitor and quantify substrate consumption and formation of relevant intermediates or products, analysis was conducted using HPLC-MS.

After adjustment of pH and temperature, HPLC-MS analysis revealed a second peak with the same mass signal as the substrate but shifted retention time (Figure 4B). This indicated the formation of the acyl N, O shifted ester intermediate followed by appearance of the desired products H-S-G-W-CONH2 and [Ga(NOTA)]. Observation of the putative structural isomer ester intermediate corroborates that amide bond hydrolysis occurs by the N, O acyl shift. NO2A-amide ligands exhibit coordination of the carbonyl oxygen (N3O3 donor set) or amide nitrogen (N4O2) with gallium, with the coordinative switch occurring between pH 3 and 5. Both coordinative modes can induce N, O acyl shift rearrangement S5,45 followed by subsequent ester hydrolysis.

The presence of two reaction mechanisms resulting in the N, O acyl shift is further supported by the uncharacteristic pH dependence of the observed reaction rates determined in

accordance with previous reports. We observed accelerated rearrangement and ester hydrolysis at pH 4.5, when compared with data acquired at 5.5 and 6.5. This is opposite of the typically observed pH dependence of N, O acyl shift-mediated autoproteolysis reactions that show the fastest reaction rates at pH 5.5–6. We note that data obtained at pH 5.5–7.5, where the N₄O₂ complex species dominates, corroborate the general trend well (Figure 4D). Hollow we cannot exclude that some amount of the substrate is hydrolyzed by attack of an exogenous nucleophilic water/OH⁻, as indicated by observed, slow turnover of G-linked test sequences vide supra, the observed pH dependence renders this process less probable and likely only a minor contributor.

Characterization of the N₃O₃ Species with VT-MS and MS-IR. In accordance with previous studies on quantification of the inner-sphere hydration of coordination complexes using variable temperature mass spectrometry (VT-MS), we carried out a corresponding analysis on the positively charged N₃O₃ species of [Ga(NO2A)]+-S-G-W-CONH₂ to probe ternary aqua complex formation in the gas phase. 48,49 We were able to exclude inner-sphere water; the binding energy was found to be -30.1 ± 2.7 kJ/mol, within the threshold of -34 kJ/mol established for inner-sphere water and consistent with the result for the metal-free NO2A-S-G-W-CONH₃⁺ (Supporting Information, Figures S58 and S60). This indicates that even at elevated pH, the complex-adjacent amide bond is not nucleophilically attacked by the inner-sphere water. Therefore, such a reaction mechanism (mechanism (i) vide supra) can likely be excluded. Furthermore, formation of a ternary aqua complex was not supported by a previous study using solidstate X-ray structural data of [Ga(NO2A-amide)]+ complexes.4

We next sought to structurally characterize the species observed in the HPLC-MS experiments using mass-selective infrared spectroscopy (MS-IR). Briefly, this technique isolates the analyte in a mass spectrometer, allowing an infrared absorption spectrum of a well-defined hydration state to be recorded. We posited that carbonyl stretches in [Ga-(NO2A)]+-S-G-W-CONH2 and its isotopically labeled analogue could be identified to provide confirmative structural assignment of the N₃O₃ motif. Figure 5 compares the spectra of NO2A-S-G-W-CONH₃⁺, [Ga(NO2A)]⁺-S-G-W-CONH₂, and [Ga(NO2A)]+-*S-G-W-CONH2, a corresponding analogue containing N-15/C-13-labeled serine (Supporting Information, Figure S63). The incorporation of the metal ion enables clear identification of the carboxy stretches at 1719 and 1767 cm⁻¹ (Figure 5, purple), following the pattern for EDTAchelated metal ions reported recently. 50 These features appear broader in the metal-free species, likely due to isomers involving different arrangements of the carboxylic acid groups in the absence of Ga. Introduction of isotopically labeled serine residues induces a distinct redshift of the 13C-carbonyl amide to lower wavenumbers (denoted by *) and provides means to assign other peptide-backbone amide carbonyl stretches (Figure 5, blue).³¹ Finally, the coordination of the amido carbonyl (Figure 5, orange) to the Ga³⁺ metal center yields a redshift and an intensity increase as expected, 52,53 and the adjacent ¹⁵N of the seryl residue further lowers the vibrational frequency in the labeled complex. These assignments are supported by quantum chemical calculations, which confirm that complexation of the carbonyl leads to an 85 cm⁻¹ redshift (Figure S106).

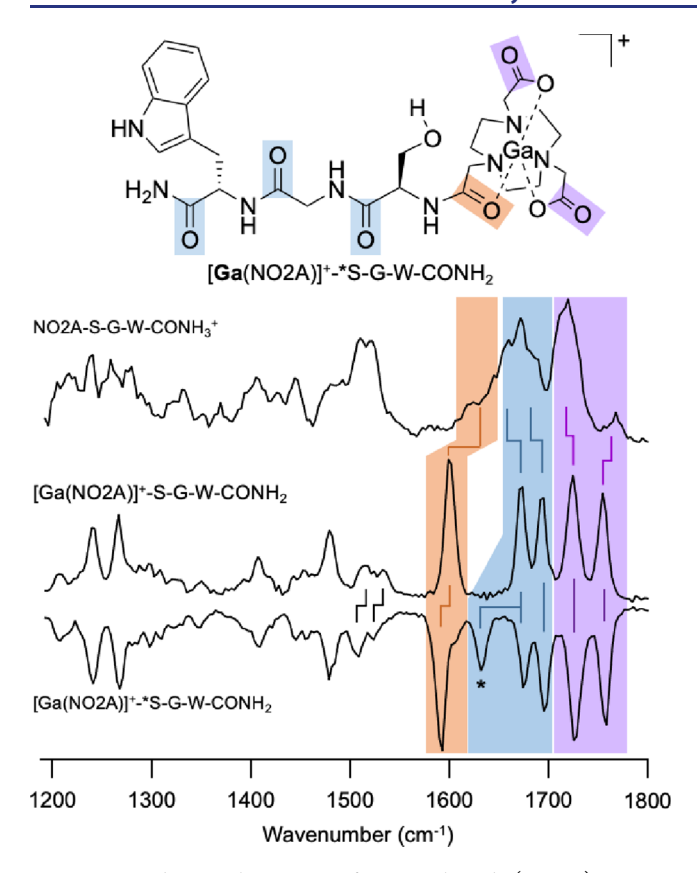


Figure 5. Vibrational spectra of mass-selected (NO2A)-S-G-W-CONH₂, the corresponding Ga complex, and the isotopically labeled analogue demonstrating clearly identifiable carbonyl stretches across the entire molecule. The coordinated carbonyl (orange) redshifts and gains intensity compared to the metal-free complex. The asterisk (*) denotes the carbonyl associated with 13 C.

With this spectroscopic signature understood, we turned to identify the structure of the intermediate. We expected the $\rm N_3O_3$ coordination mode to retain the coordinated amido carbonyl feature and the $\rm N_4O_2$ mode to lose it. Given that the $\rm N_4O_2$ complex is neutral, we observe it in the mass spectrum as a sodium adduct. Figure 6B compares the spectra of the native to the sodiated species. Sodiation yields a clear free OH stretching signal, highlighting the intact serine OH, and removes the Ga-coordinated carbonyl stretching feature, identifying this as the $\rm N_4O_2$ complex. Shifts in the free NH stretches upon sodiation are attributed to the breaking of backbone NH···OC hydrogen bonds in favor of chelation of the sodium ion by the amid carbonyls.

Having positively identified both the N₃O₃ and N₄O₂ complexes, we next tracked the changes to their spectra upon 2 h of incubation (shaded spectra in Figure 6C). No changes are observed in the spectrum of [Ga(NO2A)]+-S-G-W-CONH₃⁺, but the intensity of its signal in the mass spectrum reduces with incubation time in a similar manner to the HPLC-MS results in Figure 4. Combined with a concomitant increase in the sodium adduct signal, this suggests the depletion of N_3O_3 and production of N_4O_2 as the reaction progresses. Moving to the spectrum of the sodium adduct, much of the spectrum is similar after incubation, but the OH stretching feature (identified by "-" in Figure 6C) is substantially reduced. Further inspection of the spectrum of the isotopically enriched species reveals a simultaneous reduction of the intensity of the serine amide stretch near 3400 cm⁻¹ (also marked with "-"), which suffers a 6 cm⁻¹ redshift upon exchange with ¹⁵N. Quantum chemical predictions (Figure S106) suggest more than a hundred-fold reduction of the intensity of this NH stretch after the acyl shift. Thus, we conclude that the spectra indicate depletion of the unreacted complex and the generation of a structurally similar

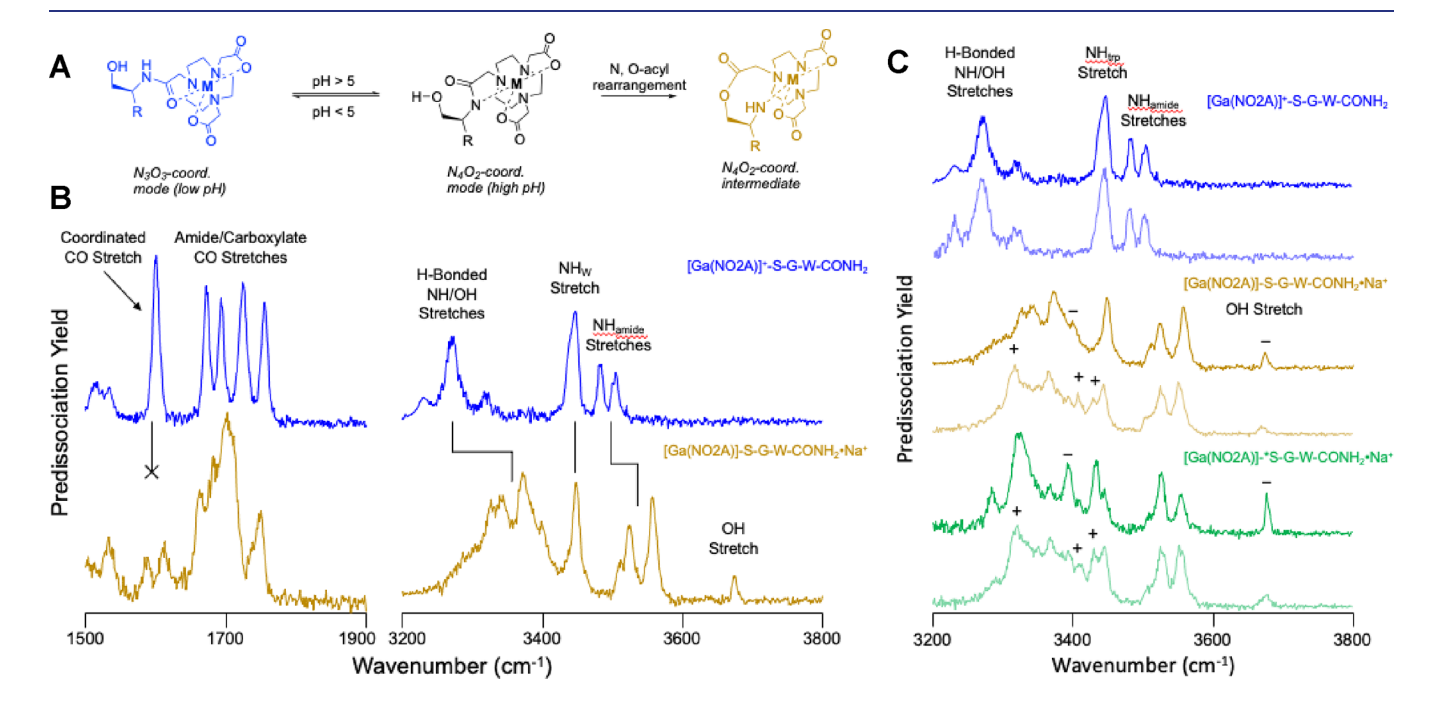


Figure 6. (A) Structures observed by MS-IR analysis. (B) IR spectra of NO2A-S-G-W-CONH₃⁺ (blue) and its sodiated reaction intermediate (gold) as prepared. (C) Spectra of as-prepared (dark) and incubated (2 h, shaded) NO2A-S-G-W-CONH₃⁺ and its sodiated intermediate (gold: monoisotopic; green: isotopically labeled). "—" denotes specific peaks that decrease in intensity upon incubation, while "+" denotes peaks that increase in intensity.

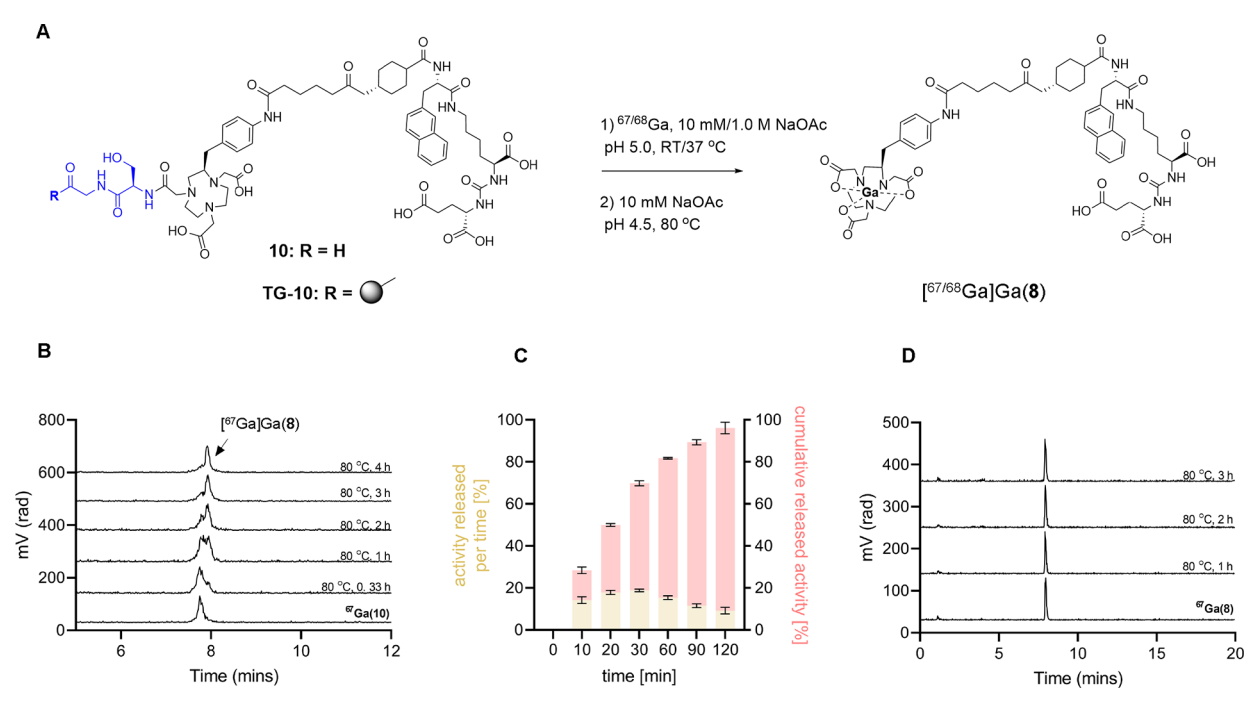


Figure 7. (A) Reaction scheme for the proof-of-concept systems based on compound 10 with amide bond cleavage in solution and on the solid phase. The cleavable sequence is shown in purple. (B) HPLC monitoring of amide bond cleavage in solution for the conversion of $^{67}Ga(10)$ to Ga(8). (C) Quantitation of the $^{68}Ga(8)$ product released from TG-10 per time (gold) and cumulative (pink). (D) Monitoring of stability of $^{67}Ga(8)$ at 80 °C demonstrating no degradation.

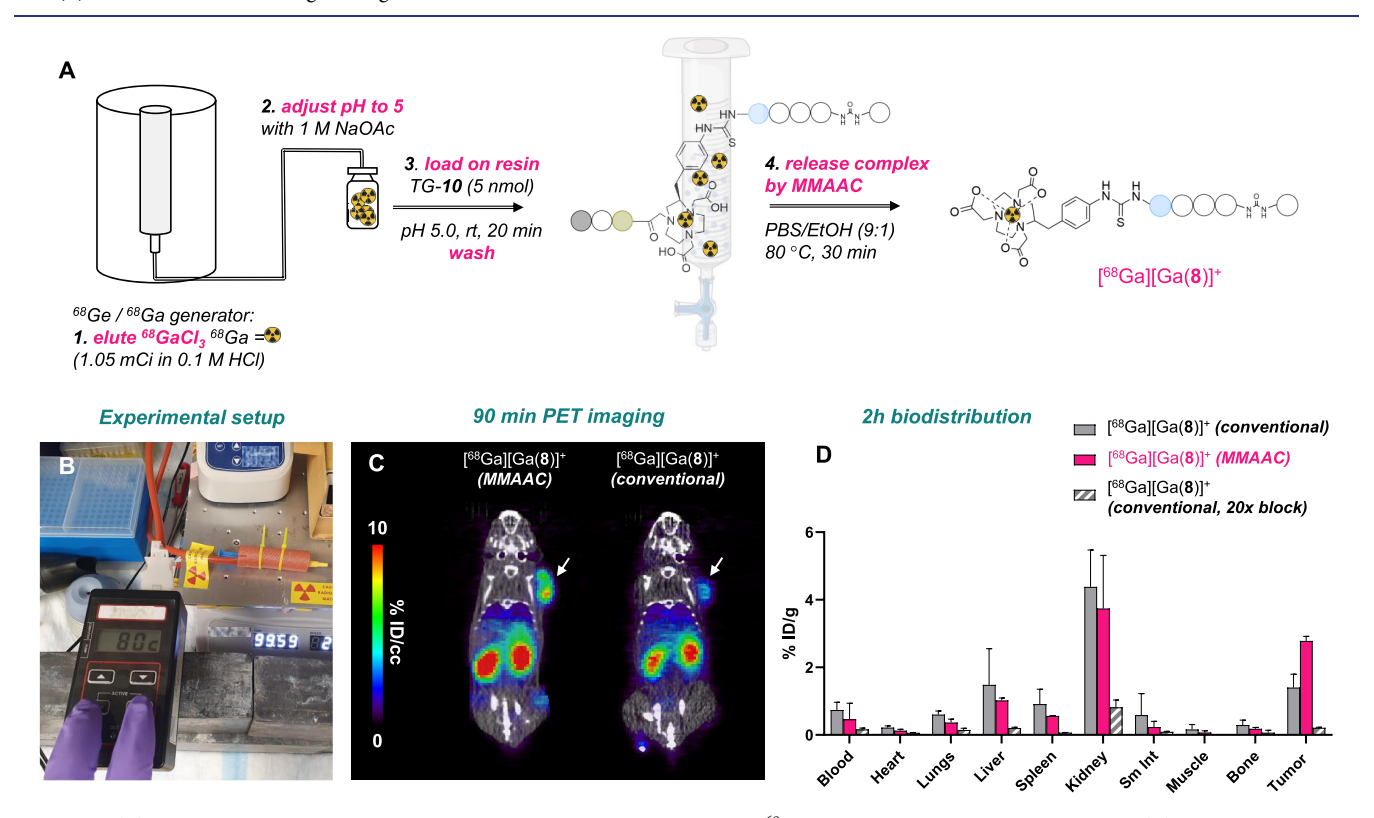


Figure 8. (A) Schematic description of MMAAC-mediated radiosynthesis of $[^{68}Ga]Ga-8$ following generator elution. (B) Photograph of the experimental setup of MMAAC with a heated syringe sleeve to induce metal-mediated hydrolysis following the chelation step. (C) Coronal PET-CT images 90 min postinjection of mice injected with 50 μ Ci $[^{68}Ga]Ga-8$ synthesized with MMAAC (left) or conventional solution-phase synthesis (right). (D) Biodistribution analysis 2 h postinjection (n=4).

species lacking OH and serine NH moieties that we identify as the acyl-shifted N_4O_2 intermediate.

Proof-of-Concept (1): Selective Release of High-Molar-Activity Radiopharmaceuticals. Subsequently, we conducted a first validation of the MMAAC strategy for

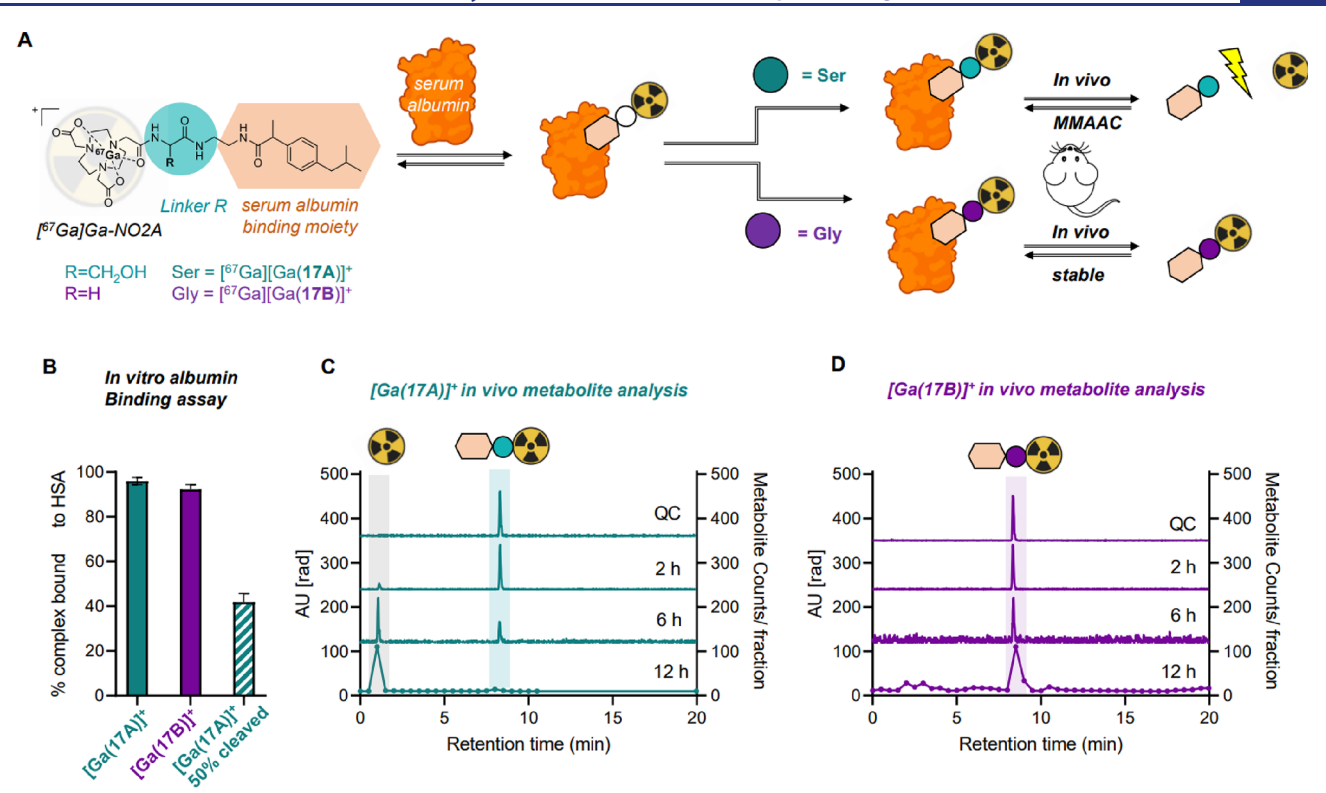


Figure 9. (A) Probe design and mechanism of action of sequence-dependent cleavage in vivo. (B) In vitro binding experiment probing binding affinity to human serum albumin (n = 3). (C) Urine metabolite analysis of $[^{67}Ga][Ga(17A)]^+$ (blue box) with an appearing target metabolite $[^{67}Ga]Ga(NOTA)$ (gray box). (D) Urine metabolite analysis of $[^{67}Ga][Ga(17B)]^+$ (purple box).

prodrug activation. To this end, we designed a [Ga(NO2A-bb-Bn)]-linked, targeted construct with a cleavable, serine—glycine prodrug cap. We prepared the NOTA-linked short peptide conjugate 10, targeting the prostate-specific membrane antigen (PSMA). The construct includes a doubly functionalized NOTA chelator that incorporates a cleavable G–S (glycine—serine) cap by amidation; a PSMA-targeting peptide was introduced via backbone functionalization of the macrocycle in accordance with methods established by us previously (Figure 7A).⁵⁴

We then probed radiochemical labeling and autocleavage efficiency with the radioactive isotope 67 Ga. The direct, insolution radiolabeling to produce $[^{67}$ Ga]Ga(10) resulted in high radiochemical yield (>90%) at pH 5.0 and at 37 °C. Incubation of $[^{67}$ Ga]Ga(10) at 37 and 80 °C revealed the selective release of 67 Ga-NOTA-Bn-PSMA ($[^{67}$ Ga]Ga(8)) with $t_{1/2}=22.2$ and 0.81 h, respectively (Figure 7B and Supporting Information, Figure S64). The resulting product $[^{67}$ Ga]Ga(8) was not sensitive to further degradation or radiolysis within 80 h at 80 °C (Figure 7D and Supporting Information, Figure S64). The significantly accelerated amide bond cleavage even at 37 °C indicates that the autolytic amide bond cleavage mechanism can be modulated by greater steric encumbrance and may be compatible with prodrug activation by release in vivo systems.

With these optimized drug release conditions validated in solution, we posited that selective release of radiopharmaceuticals from a solid support upon binding of the metal ion would be feasible. If successfully implemented, MMAAC would result in the release of only the desired radiometal complex into solution, while the unreacted precursor would remain on the solid support, maximizing achievable molar activities. This

contrasts with conventional, in-solution radiochelation, which produces the radiolabeled complex in the presence of a 4–5 orders of magnitude excess ligand (e.g., typically a 1:1000 M:L ratio), limiting achievable molar activities, which consequently can inhibit or reduce effective binding of in vivo targets. ⁵⁵

The synthesis of the tentagel-appended PSMA-NOTA (TG-10) prodrug was conducted using a postsynthetic, terminal resin loading strategy (see the Supporting Information). To validate MMAAC as an efficient strategy for preparation of radiopharmaceuticals, we prepared the ⁶⁸Ga-PSMA derivative ([68Ga]Ga-8) by selective release from a resin-appended prodrug using ⁶⁸Ga sourced from a commercial ⁶⁸Ge/⁶⁸Ga generator. The [⁶⁸Ga]Ga-8 radiotracer was tested for radiochemical labeling efficiency, radiochemical purity, and autocleavage efficiency using the tentagel-appended PSMA-NOTA (TG-10) prodrug. To this end, a commercial ⁶⁸Ge/⁶⁸Ga generator was eluted, buffered to pH 5, and loaded directly onto the functionalized resin TG-10 in at a total reaction volume of 1 mL. Radiolabeling was conducted at 37 °C using 10 nmol of the peptide on resin (Figures 7A and 8A). The direct solid-phase radiolabeling step retained >90% of the loaded activity. Subsequent incubation of TG-10 at 80 °C produced [68 Ga]Ga(NOTA)-Bn-PSMA ([68 Ga]Ga-8) with $t_{1/2}$ = 0.5 h (Figure 7C) and efficient release of >95% of bound activity from the resin. The resulting product was hydrolytically stable at 80 °C (Figure 7D). Coregistration of the UV signal with the resin-eluate indicates that the quantity of the released peptide is too low to be detectable, which is in accordance with the anticipated high molar activity of the product.

To validate the performance of the high-molar-activity construct, we tested $[^{68}Ga][Ga(8)]$ in a corresponding mouse

model. Specifically, we employed the RM-1 murine prostate cancer cell line compatible with immunocompetent mice. In contrast with the human-derived PSMA-expressing cell lines PC-3 PiP (500,000 receptor copies per cell), RM-1 only expresses approximately 80,000 copies of the PSMA receptor per cell. 56,57 This induces a greater sensitivity to the molar activity of radiopharmaceuticals, with low molar activity reducing probe uptake in target tissues. We conducted radiosynthesis of [68Ga]Ga-8 using MMAAC followed by administration to tumor-bearing mice, positron emission tomography (PET) imaging at 90 min postinjection, and biodistribution analysis at 2 h postinjection. Uptake in the tumor reached 2.45% ID/g at 2 h postinjection, demonstrating good tumor conspicuity and significant target accumulation (Figure 8C,D, "MMAAC", pink bars). Comparatively, when we conducted a conventional, in-solution radiosynthesis, imaging, and biodistribution analysis with 0.2 mCi/nmol molar activity, probe accumulation reached only 0.97% ID/g in the tumor (Figure 8C,D, "conventional", gray bars). A corresponding blocking experiment at 0.01 mCi/nmol molar activity further demonstrated the reduction of target-specific uptake and sensitivity of this cell line and tumor model to the radiopharmaceuticals' molar activity (Figure 8D, striped bars).

Proof-of-Concept (2): Prodrug Release In Vivo. Due to the feasibility of MMAAC at 37 °C, we posited that the hydrolysis of the metal complex could also be observed in vivo. To this end, we designed proof-of-concept constructs 17 and 18, which incorporate the $[M(NO2A)]^{n+}$ -X (X = G or S) motif appended to en-ibuprofen. This moiety has previously shown to bind effectively to murine and human serum albumin^{58,59} and thus would exhibit prolonged in vivo circulation to track reaction progress using radiochemical tracing with the longerlived isotope ⁶⁷Ga (Figure 9A). In-solution chemical synthesis of 17A (X = S, cleavable) and 17B (X = G, noncleavable)control) was achieved by sequential solution phase amide bond couplings (Supporting Information). Sensitivity to hydrolysis of [Ga(17A)]+ was verified, and the human serum-albumin (HSA) binding of [67Ga][Ga(17A)]⁺ and [67Ga][Ga(17B)]⁺ was 96 and 92%, respectively (Figure 9B). Hydrolysis of 50% [67Ga][Ga(17A)]+ resulted in 42% bound activity to HSA, demonstrating that the hydrolyzed complex [67Ga]Ga(NOTA) did not exhibit significant binding (Figure 8B).

With $[^{67}Ga][Ga(17A)]^+$ and $[^{67}Ga][Ga(17B)]^+$ validated, we conducted in vivo metabolite tracking experiments next. The constructs (200 μ Ci) were administered to separate cohorts of naïve balb/C mice, and cohorts (n = 3) were sacrificed at 2, 6, 12, and 24 h postinjection. In addition to biodistribution, blood and urine metabolite analysis was conducted with radio-HPLC, as intact probes and hydrolyzed complex metabolites are easily distinguishable by retention time. We observed effective MMAAC release of the [67Ga]-Ga(NOTA) complex for [67Ga][Ga(17A)]+ in blood and urine (Figure 9C), while [67Ga][Ga(17B)]+ was stable and appeared as the only detectable metabolite at sampled time points (Figure 9D). In contrast with previously determined kinetic rates ex vivo, [⁶⁷Ga][Ga(17A)]⁺ was fully hydrolyzed at the 12 h mark, which indicates that in vivo hydrolysis proceeds with a significantly faster rate than in the test tube. We currently hypothesize that the more lipophilic protein environment of serum albumin accelerates the MMAAC rate when $[^{67}Ga][Ga(17A)]^+$ is bound; future experiments beyond the scope of this work are planned to address and further study

how MMAAC rates can be modulated selectively in vitro and in vivo.

CONCLUSIONS

In summary, we demonstrate autolytic, metal complex-mediated amide bond cleavage, which represents a viable method for prodrug activation and synthesis of metallodrugs. The activation of corresponding prodrug structures by the N, O acyl shift mechanism occurs only following formation of the corresponding coordination complex. Conveniently, reaction rates remain (too) slow at room temperature and significantly accelerate at elevated temperatures (37/80 °C) The strict dependence of the observed reactivity on direct adjacency to serine provides a convenient tool to build clearly defined prodrug structures that employ metal complexes as release triggers.

The MMAAC approach is compatible with trace concentrations of the prodrug and metal ions without the need for an exogenous catalyst or reactant to produce the desired product, as demonstrated by studies conducted at the macroscopic (µmol) and radiotracer (pmol) scale. Our corresponding proof-of-concept studies indicate that autolytic, metal complexmediated amide bond cleavage is suitable for the synthesis of "slow-release" and high-specific-activity radiopharmaceuticals: two in vivo experiments were carried out to demonstrate that (1) high-molar-activity radiopharmaceuticals synthesized with MMAAC can exhibit improved in vivo performance and (2) MMAAC can be employed to induce selective compound degradation in vivo. Future work will entail expansion of scope beyond Ga³⁺ and Sc³⁺ metal ions and tuning of reaction rates by modification of the peptide sequence, ionic strength, and polarity of the chemical environment.

ASSOCIATED CONTENT

Supporting Information

The Supporting Information is available free of charge at https://pubs.acs.org/doi/10.1021/jacs.3c05492.

Detailed experimental procedures, NMR, HRMS, and HPLC results; characterization of complexes and radiolabeling data (PDF)

AUTHOR INFORMATION

Corresponding Author

Eszter Boros — Department of Chemistry, Stony Brook University, Stony Brook, New York 11794, United States; Department of Chemistry, University of Wisconsin-Madison, Madison, Wisconsin 53706, United States; oorcid.org/ 0000-0002-4186-6586; Email: eboros@wisc.edu

Authors

Dariusz Śmilowicz – Department of Chemistry, Stony Brook University, Stony Brook, New York 11794, United States; Department of Chemistry, University of Wisconsin-Madison, Madison, Wisconsin 53706, United States

Shawn Eisenberg — Department of Chemistry, Stony Brook University, Stony Brook, New York 11794, United States Rochelle LaForest — Department of Chemistry, Stony Brook University, Stony Brook, New York 11794, United States

Jennifer Whetter — Department of Chemistry, Stony Brook University, Stony Brook, New York 11794, United States; Department of Chemistry, University of Wisconsin-Madison, Madison, Wisconsin 53706, United States

- Annapoorani Hariharan Department of Chemistry, Stony Brook University, Stony Brook, New York 11794, United States
- Jake Bordenca Department of Chemistry, Stony Brook University, Stony Brook, New York 11794, United States Christopher J. Johnson — Department of Chemistry, Stony Brook University, Stony Brook, New York 11794, United States; © orcid.org/0000-0003-1859-5615

Complete contact information is available at: https://pubs.acs.org/10.1021/jacs.3c05492

Funding

E.B. acknowledges the Gordon & Betty Moore foundation for generous support of this work through the 2020 Moore Fellowship and the National Institutes of Health (R01EB032349-01A1). C.J.J. acknowledges the National Science Foundation (NSF), CHE-1905172.

Notes

The authors declare no competing financial interest.

ACKNOWLEDGMENTS

Nicoline Frederiks is acknowledged for support with mass spectrometry and spectroscopy data acquisition.

REFERENCES

- (1) Twilton, J.; Le, C. C.; Zhang, P.; Shaw, M. H.; Evans, R. W.; MacMillan, D. W. The merger of transition metal and photocatalysis. *Nat. Rev. Chem.* **2017**, *1*, 1–19.
- (2) Lee, M.; Maji, B.; Manna, D.; Kahraman, S.; Elgamal, R. M.; Small, J.; Kokkonda, P.; Vetere, A.; Goldberg, J. M.; Lippard, S. J.; Kulkarni, R. N.; Wagner, B. K.; Choudhary, A. Native zinc catalyzes selective and traceless release of small molecules in β -cells. *J. Am. Chem. Soc.* **2020**, 142, 6477–6482.
- (3) Bolitho, E. M.; Sanchez-Cano, C.; Shi, H.; Quinn, P. D.; Harkiolaki, M.; Imberti, C.; Sadler, P. J. Single-cell chemistry of photoactivatable platinum anticancer complexes. *J. Am. Chem. Soc.* **2021**, *143*, 20224–20240.
- (4) Alonso-de Castro, S.; Ruggiero, E.; Ruiz-de-Angulo, A.; Rezabal, E.; Mareque-Rivas, J. C.; Lopez, X.; López-Gallego, F.; Salassa, L. Riboflavin as a bioorthogonal photocatalyst for the activation of a Pt IV prodrug. *Chem. Sci.* **2017**, *8*, 4619–4625.
- (5) Sun, Y.; Frenkel-Pinter, M.; Liotta, C. L.; Grover, M. A. The pH dependent mechanisms of non-enzymatic peptide bond cleavage reactions. *PCCP* **2020**, 22, 107–113.
- (6) Yu, B.; Zheng, Y.; Yuan, Z.; Li, S.; Zhu, H.; De La Cruz, L. K.; Zhang, J.; Ji, K.; Wang, S.; Wang, B. Toward direct protein Spersulfidation: a prodrug approach that directly delivers hydrogen persulfide. *J. Am. Chem. Soc.* **2018**, *140*, 30–33.
- (7) Wang, X.; Wang, X.; Jin, S.; Muhammad, N.; Guo, Z. Stimuli-responsive therapeutic metallodrugs. *Chem. Rev.* **2019**, *119*, 1138–1192.
- (8) Folk, D. S.; Franz, K. J. A prochelator activated by β -secretase inhibits $A\beta$ aggregation and suppresses copper-induced reactive oxygen species formation. *J. Am. Chem. Soc.* **2010**, *132*, 4994–4995.
- (9) Graf, N.; Lippard, S. J. Redox activation of metal-based prodrugs as a strategy for drug delivery. *Adv. Drug Delivery Rev.* **2012**, *64*, 993–1004
- (10) Guo, Z.; Hong, H.; Zheng, Y.; Wang, Z.; Ding, Z.; Fu, Q.; Liu, Z. Radiotherapy-Induced Cleavage of Quaternary Ammonium Groups Activates Prodrugs in Tumors. *Angew. Chem., Int. Ed.* **2022**, *61*, No. e202205014.
- (11) Jacobsen, F. E.; Lewis, J. A.; Cohen, S. M. A new role for old ligands: discerning chelators for zinc metalloproteinases. *J. Am. Chem. Soc.* **2006**, *128*, 3156–3157.
- (12) Yuan, Y.; Zhang, C.-J.; Liu, B. A platinum prodrug conjugated with a photosensitizer with aggregation-induced emission (AIE)

- characteristics for drug activation monitoring and combinatorial photodynamic—chemotherapy against cisplatin resistant cancer cells. *Chem. Commun.* **2015**, *51*, 8626—8629.
- (13) Zhao, Z.; Tao, X.; Xie, Y.; Lai, Q.; Lin, W.; Lu, K.; Wang, J.; Xia, W.; Mao, Z. W. In Situ Prodrug Activation by an Affibody-Ruthenium Catalyst Hybrid for HER2-Targeted Chemotherapy. *Angew. Chem., Int. Ed.* **2022**, *61*, No. e202202855.
- (14) Velema, W. A.; Szymanski, W.; Feringa, B. L. Photopharmacology: beyond proof of principle. *J. Am. Chem. Soc.* **2014**, 136. 2178–2191.
- (15) Gawne, P. J.; Man, F.; Blower, P. J.; TM de Rosales, R. Direct Cell Radiolabeling for in Vivo Cell Tracking with PET and SPECT Imaging. *Chem. Rev.* **2022**, *122*, 10266–10318.
- (16) Oliveira, B. L.; Stenton, B. J.; Unnikrishnan, V.; de Almeida, C. t. R.; Conde, J. o.; Negrão, M.; Schneider, F. S.; Cordeiro, C.; Ferreira, M. G.; Caramori, G. F.; Domingos, J. B.; Fior, R.; Bernardes, G. J. L. Platinum-triggered bond-cleavage of pentynoyl amide and N-propargyl handles for drug-activation. *J. Am. Chem. Soc.* **2020**, *142*, 10869–10880.
- (17) Zhang, X.; Smith, R. T.; Le, C.; McCarver, S. J.; Shireman, B. T.; Carruthers, N. I.; MacMillan, D. W. Copper-mediated synthesis of drug-like bicyclopentanes. *Nature* **2020**, *580*, 220–226.
- (18) Sabatino, V.; Rebelein, J. G.; Ward, T. R. "Close-to-release:" spontaneous bioorthogonal uncaging resulting from ring-closing metathesis. J. Am. Chem. Soc. 2019, 141, 17048–17052.
- (19) Sabatino, V.; Unnikrishnan, V.; Bernardes, G. J. Transition metal mediated bioorthogonal release. *Chem Catal.* **2022**, *2*, 39–51.
- (20) Wang, X.; Liu, Y.; Fan, X.; Wang, J.; Ngai, W. S. C.; Zhang, H.; Li, J.; Zhang, G.; Lin, J.; Chen, P. R. Copper-triggered bioorthogonal cleavage reactions for reversible protein and cell surface modifications. *J. Am. Chem. Soc.* **2019**, *141*, 17133–17141.
- (21) Hsu, H.-T.; Trantow, B. M.; Waymouth, R. M.; Wender, P. A. Bioorthogonal catalysis: a general method to evaluate metal-catalyzed reactions in real time in living systems using a cellular luciferase reporter system. *Bioconjugate Chem.* **2016**, *27*, 376–382.
- (22) van Rixel, V. H.; Ramu, V.; Auyeung, A. B.; Beztsinna, N.; Leger, D. Y.; Lameijer, L. N.; Hilt, S. T.; Le Dévédec, S. E.; Yildiz, T.; Betancourt, T. Photo-uncaging of a microtubule-targeted rigidin analogue in hypoxic cancer cells and in a xenograft mouse model. *J. Am. Chem. Soc.* 2019, 141, 18444—18454.
- (23) Cole, H. D.; Roque, J. A., III; Shi, G.; Lifshits, L. M.; Ramasamy, E.; Barrett, P. C.; Hodges, R. O.; Cameron, C. G.; McFarland, S. A. Anticancer Agent with Inexplicable Potency in Extreme Hypoxia: Characterizing a Light-Triggered Ruthenium Ubertoxin. *J. Am. Chem. Soc.* **2022**, *144*, 9543–9547.
- (24) Roque, J. A., III; Cole, H. D.; Barrett, P. C.; Lifshits, L. M.; Hodges, R. O.; Kim, S.; Deep, G.; Francés-Monerris, A.; Alberto, M. E.; Cameron, C. G. Intraligand Excited States Turn a Ruthenium Oligothiophene Complex into a Light-Triggered Ubertoxin with Anticancer Effects in Extreme Hypoxia. *J. Am. Chem. Soc.* 2022, 144, 8317–8336.
- (25) Chang, T. C.; Vong, K.; Yamamoto, T.; Tanaka, K. Prodrug Activation by Gold Artificial Metalloenzyme-Catalyzed Synthesis of Phenanthridinium Derivatives via Hydroamination. *Am. Ethnol.* **2021**, 133, 12554–12562.
- (26) Neumann, K.; Gambardella, A.; Lilienkampf, A.; Bradley, M. Tetrazine-mediated bioorthogonal prodrug-prodrug activation. *Chem. Sci.* **2018**, *9*, 7198–7203.
- (27) Vanjari, R.; Panda, D.; Mandal, S.; Vamisetti, G. B.; Brik, A. Gold (I)-Mediated Rapid Cyclization of Propargylated Peptides via Imine Formation. *J. Am. Chem. Soc.* **2022**, *144*, 4966–4976.
- (28) Bray, T. L.; Salji, M.; Brombin, A.; Pérez-López, A. M.; Rubio-Ruiz, B.; Galbraith, L. C.; Patton, E. E.; Leung, H. Y.; Unciti-Broceta, A. Bright insights into palladium-triggered local chemotherapy. *Chem. Sci.* **2018**, *9*, 7354–7361.
- (29) McCall, K. A.; Huang, C.-c.; Fierke, C. A. Function and mechanism of zinc metalloenzymes. *J. Nutr.* **2000**, *130*, 1437S—1446S.

- (30) Fernandez-Patron, C.; Stewart, K. G.; Zhang, Y.; Koivunen, E.; Radomski, M. W.; Davidge, S. T. Vascular matrix metalloproteinase-2-dependent cleavage of calcitonin gene-related peptide promotes vasoconstriction. Circ. Res. 2000, 87, 670-676.
- (31) Gao, L.; Zhang, Y.; Zhao, L.; Niu, W.; Tang, Y.; Gao, F.; Cai, P.; Yuan, Q.; Wang, X.; Jiang, H.; Gao, X. An artificial metalloenzyme for catalytic cancer-specific DNA cleavage and operando imaging. Sci. Adv. 2020, 6, No. eabb1421.
- (32) Groves, J. T.; Baron, L. A. Models of zinc-containing proteases. Catalysis of cobalt (III)-mediated amide hydrolysis by a pendant carboxylate. J. Am. Chem. Soc. 1989, 111, 5442-5448.
- (33) Kita, Y.; Nishii, Y.; Higuchi, T.; Mashima, K. Zinc-Catalyzed Amide Cleavage and Esterification of β -Hydroxyethylamides. *Angew.* Chem., Int. Ed. Engl. 2012, 124, 5821-5824.
- (34) Hegg, E. L.; Burstyn, J. N. Hydrolysis of unactivated peptide bonds by a macrocyclic copper (II) complex: Cu ([9] aneN3) Cl2 hydrolyzes both dipeptides and proteins. J. Am. Chem. Soc. 1995, 117, 7015-7016.
- (35) Krezel, A.; Kopera, E.; Protas, A. M.; Poznański, J.; Wysłouch-Cieszyńska, A.; Bal, W. Sequence-specific Ni (II)-dependent peptide bond hydrolysis for protein engineering. Combinatorial library determination of optimal sequences. J. Am. Chem. Soc. 2010, 132, 3355-3366.
- (36) Wezynfeld, N. E.; Frączyk, T.; Bonna, A.; Bal, W. Peptide bond cleavage in the presence of Ni-containing particles. Metallomics 2020, 12, 649-653.
- (37) Ho, P. H.; Mihaylov, T.; Pierloot, K.; Parac-Vogt, T. N. Hydrolytic activity of vanadate toward serine-containing peptides studied by kinetic experiments and dft theory. Inorg. Chem. 2012, 51,
- (38) Wezynfeld, N. E.; Fraczyk, T.; Bal, W. Metal assisted peptide bond hydrolysis: Chemistry, biotechnology and toxicological implications. Coord. Chem. Rev. 2016, 327, 166-187.
- (39) Yang, Y.; Lu, C.; Wang, H.; Liu, X. Amide bond cleavage initiated by coordination with transition metal ions and tuned by an auxiliary ligand. Dalton Trans. 2016, 45, 10289-10296.
- (40) Jbara, M.; Eid, E.; Brik, A. Gold (I)-mediated decaging or cleavage of propargylated peptide bond in aqueous conditions for protein synthesis and manipulation. J. Am. Chem. Soc. 2020, 142,
- (41) Latocheski, E.; Dal Forno, G. M.; Ferreira, T. M.; Oliveira, B. L.; Bernardes, G. J.; Domingos, J. B. Mechanistic insights into transition metal-mediated bioorthogonal uncaging reactions. Chem. Soc. Rev. 2020, 49, 7710-7729.
- (42) Majkowska-Pilip, A.; Bilewicz, A. Macrocyclic complexes of scandium radionuclides as precursors for diagnostic and therapeutic radiopharmaceuticals. J. Inorg. Biochem. 2011, 105, 313-320.
- (43) Kopera, E.; Krezel, A.; Protas, A. M.; Belczyk, A.; Bonna, A.; Wysłouch-Cieszyńska, A.; Poznański, J.; Bal, W. Sequence-specific Ni (II)-dependent peptide bond hydrolysis for protein engineering: reaction conditions and molecular mechanism. Inorg. Chem. 2010, 49, 6636-6645.
- (44) Shetty, D.; Choi, S. Y.; Jeong, J. M.; Hoigebazar, L.; Lee, Y. S.; Lee, D. S.; Chung, J. K.; Lee, M. C.; Chung, Y. K. Formation and Characterization of Gallium (III) Complexes with Monoamide Derivatives of 1, 4, 7-Triazacyclononane-1, 4, 7-triacetic Acid: A Study of the Dependency of Structure on Reaction pH. Eur. J. Inorg. Chem. 2010, 34, 5432-5438.
- (45) Ho, P. H.; Stroobants, K.; Parac-Vogt, T. N. Hydrolysis of serine-containing peptides at neutral pH promoted by [MoO4] 2oxyanion. Inorg. Chem. 2011, 50, 12025-12033.
- (46) Shao, Y. Protein splicing: estimation of the rate of O-N and S-N acyl rearrangements, the last step of the splicing process. J. Pept. Res. 1997, 50, 193-198.
- (47) Johansson, D. G.; Wallin, G. r.; Sandberg, A.; Macao, B.; Åqvist, J.; Härd, T. Protein autoproteolysis: conformational strain linked to the rate of peptide cleavage by the pH dependence of the N O acyl shift reaction. J. Am. Chem. Soc. 2009, 131, 9475-9477.

- (48) Racow, E. E.; Kreinbihl, J. J.; Cosby, A. G.; Yang, Y.; Pandey, A.; Boros, E.; Johnson, C. J. A General Approach to Direct Measurement of the Hydration State of Coordination Complexes: Variable Temperature Mass Spectrometry. J. Am. Chem. Soc. 2019, 141, 14650-14660.
- (49) Vaughn, B.; Koller, A.; Chen, Z.; Ahn, S. H.; Loveless, C.; Cingoranelli, S.; Yang, Y.; Cirri, A.; Johnson, C.; Lapi, S.; Chapman, K.; Boros, E. Enforcing Homologous Structural, Chemical and Biological Behavior of Sc and Lu Isotopes using Restrictive Chelate Architecture. Bioconjugate Chem. 2021, 32, 1232-1241.
- (50) Foreman, M. M.; Weber, J. M. Ion Binding Site Structure and the Role of Water in Alkaline Earth EDTA Complexes. J. Phys. Chem. Lett. 2022, 13, 8558-8563.
- (51) Garand, E.; Kamrath, M. Z.; Jordan, P. A.; Wolk, A. B.; Leavitt, C. M.; McCoy, A. B.; Miller, S. J.; Johnson, M. A. Determination of Noncovalent Docking by Infrared Spectroscopy of Cold Gas-Phase Complexes. Science 2012, 335, 694-698.
- (52) Meyer, K. A. E.; Nickson, K. A.; Garand, E. The impact of the electric field of metal ions on the vibrations and internal hydrogen bond strength in alkali metal ion di- and triglycine complexes. J. Chem. Phys. 2022, 157, 174301.
- (53) Seco, M. Acetylacetone: A versatile ligand. J. Chem. Educ. 1989, 66, 779.
- (54) Smiłowicz, D.; Schlyer, D.; Boros, E.; Meimetis, L. Evaluation of a Radio-IMmunoStimulant (RIMS) in a Syngeneic Model of Murine Prostate Cancer and ImmunoPET Analysis of T-cell Distribution. Mol. Pharmaceutics 2022, 19, 3217-3227.
- (55) Eder, M.; Neels, O.; Müller, M.; Bauder-Wüst, U.; Remde, Y.; Schäfer, M.; Hennrich, U.; Eisenhut, M.; Afshar-Oromieh, A.; Haberkorn, U.; Kopka, K. Novel preclinical and radiopharmaceutical aspects of [68Ga]Ga-PSMA-HBED-CC: A new PET tracer for imaging of prostate cancer. Pharmaceuticals 2014, 7, 779-796.
- (56) Fendler, W. P.; Stuparu, A. D.; Evans-Axelsson, S.; Lückerath, K.; Wei, L.; Kim, W.; Poddar, S.; Said, J.; Radu, C. G.; Eiber, M.; Czernin, J.; Slavik, R.; Herrmann, K. Establishing 177Lu-PSMA-617 radioligand therapy in a syngeneic model of murine prostate cancer. J. Nucl. Med. 2017, 58, 1786-1792.
- (57) Smiłowicz, D.; Schlyer, D.; Boros, E.; Meimetis, L. Evaluation of a Radio-IMmunoStimulant (RIMS) in a Syngeneic Model of Murine Prostate Cancer and ImmunoPET Analysis of T-cell Distribution. Mol. Pharmaceutics 2022, 19, 3217-3227.
- (58) Boros, E.; Caravan, P. Structure-Relaxivity Relationships of Serum Albumin Targeted MRI Probes Based on a Single Amino Acid Gd Complex. J. Med. Chem. 2013, 56, 1782-1786.
- (59) Deberle, L. M.; Benešová, M.; Umbricht, C. A.; Borgna, F.; Büchler, M.; Zhernosekov, K.; Schibli, R.; Müller, C. Development of a new class of PSMA radioligands comprising ibuprofen as an albumin-binding entity. Theranostics 2020, 10, 1678.